Realistic micromechanical modeling and simulation of boron modified titanium alloys

Arun Sreeranganathan[1], Scott. I. Lieberman[1], Harpreet Singh[1], Arun M. Gokhale[1], and Sesh Tamirisakandala[2]

[1]School of Materials Science & Engineering, Georgia Institute of Technology, Atlanta, GA

[2]Department of Mechanical Engineering, Ohio University, Athens, OH

Abstract: Finite element simulations of micro-mechanical response are performed on real and computer simulated microstructures of boron modified titanium alloys containing in-situ formed Titanium Boride (TiB) phase. The microstructure model incorporates realistic particle TiB whisker morphologies/shapes and anisotropic whisker orientations. Local constitutive properties of the Ti-6Al-4V matrix are obtained using micro-indentation technique combined with an ABAQUS model of the indentation experiment. Surface-to-surface contact with finite sliding is used to model the interaction between the Vickers indenter and the sample. The computed constitutive equations are then used in 2-D and 3-D microstructural models with realistic phase morphologies/spatial distribution to simulate the global elastic-plastic mechanical response of the composite. The results are compared with the experimental data.

Keywords: Indentation, Microstructure, Composites.

1. Introduction

Correlation of material microstructures with their macroscopic properties is of fundamental importance to materials scientists for understanding the vast spectrum of existing materials as well as for developing new materials. Material microstructures, often a complex ensemble of defects and multiple phases resulting from the processing of the material, directly affect the properties and thereby, the usability of the material. Accordingly, modeling and simulation of microstructures are becoming increasingly important due to the thrust towards accurate prediction of materials behavior under external stimuli and the design of new materials with desired properties. The success of such modeling efforts depends to a large extent on the right choice of relevant features from the microstructure under consideration as well as realistic representation of such microstructures in the models. The mechanical response of materials to external stimuli is dictated by a multitude of microstructural features, and interactions among them, spanning over length scales ranging from a few nanometers to meters. In general, the length scales in a microstructure can be divided into nano- (atomic bonds, molecular dynamics), micro- (inclusions, particles) and macro-levels (component size). From a structural point of view, the macroscopic properties of a given material are most easily influenced by the geometric and spatial attributes of microstructural features in the micro-level (grain size, spatial distribution of second phase particles, etc.). The prediction of macroscopic mechanical constitutive behavior based on the microscale attributes of a material, the so-called 'homogenization' procedure, has been an area of intensive research for the last several decades. Developments in numerical approaches such as finite element method (FEM) along with the availability of increased computational power have resulted in the use of numerical methods as the preferred approach in the modeling and simulation of material behavior. Early numerical analyses of multiphase materials have followed a unit cell approach (Bao, 1991), which assumes the microstructure to be periodic with repeating unit cells containing simple idealized particle/feature shapes such as circles and ellipses in two-dimensions and spheres and ellipsoids in three-dimensions. While such studies are useful for semi-quantitative parametric studies on the effect of first order properties of microstructure (volume fraction, average size, etc.) on the material properties, they are not likely to be useful for quantitative prediction of the mechanical and physical properties of complex real material microstructures. An alternate approach involves implementing real 2D/3D material microstructures in FE simulations (Gokhale, 1999). Though a direct interpretation of the geometry of different features in microstructures is possible by incorporating metallographic images in simulation studies, this approach suffers from the inability to provide any information on how to improve the properties of a given material. In other words, such simulations based on real microstructural cutouts are useful only for mimicking the mechanical response of a material that already exists. Parametric studies using realistic phase geometries are necessary for real structure simulations to be of use in material development studies. A systematic methodology for incorporation of realistic complex particle/feature shapes and morphologies in a computer simulated microstructure that can serve as an RVE in the computational models and simulations of mechanical properties of materials has been recently developed at the authors' group in Georgia Tech (Singh, 2006). In this contribution, FE simulations of the mechanical response of realistic microstructures of Ti-6Al-4V-1B alloy containing in-situ formed TiB whiskers are performed and are compared with experimental results. All the FE analyses were carried out using ABAQUS/STANDARD 6.6-1 for linux/x86-64 platform (openSUSE 10.2) running on a Dell Precision workstation 670 with dual 3.2GHz Intel Xeon EM64T processors and 8GB of physical memory. HP-MPI 2.2.0 packaged with the ABAQUS product CD was used for parallel execution.

2. Material and processing

The experiments were performed on Ti-6Al-4V-1B alloy (all compositions are in weight percent) produced via a pre-alloyed powder metallurgy approach at Crucible Research Corporation, Pittsburgh, Pennsylvania. In this process, a liquid melt of Ti-6Al-4V containing boron was rapidly solidified using inert gas atomization to produce Ti-6Al-4V-1B powder. The Ti-6Al-4V-1B powder of –100 mesh size (average particle size of 150 μm) was packed inside a thick-walled can of Ti-6Al-4V, vacuum outgassed at 300°C for 24 h, and sealed. The can was heated to 1,200°C, soaked for 1 h, and then blind die compacted in an extrusion chamber heated to 260°C. The billet height was reduced by about 30% at a ram speed of 6.35 mm s^{-1}, and the compact was held at a pressure of 1,400 MPa for 180 s and subsequently air-cooled to room temperature. A second billet blind die compacted by the same method was subsequently hot extruded at 1,100°C with an extrusion ratio of 16.5:1, at a ram speed of 6.35 mm s^{-1}, and air-cooled to room temperature. Specimens were sectioned from the compacted billet and extruded rod, and were prepared for metallographic observations using standard grinding and polishing techniques to obtain a final surface finish of ~0.05 µm. Figure1 shows the typical microstructure of an extruded Ti-6Al-4V-1B alloy with the in-situ formed TiB whiskers aligned along the extrusion direction.

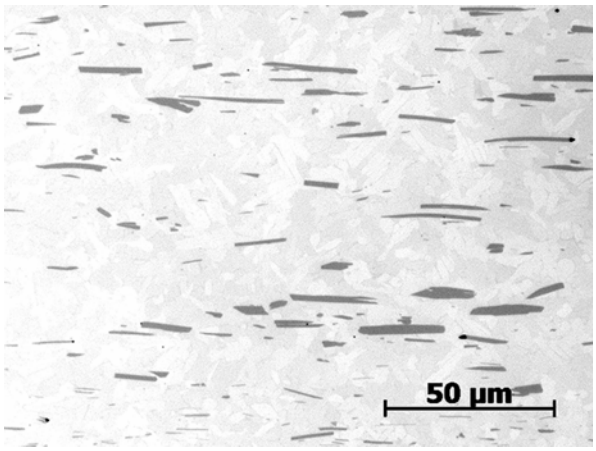

Figure 1. Typical microstructure of extruded Ti-6Al-4V-1B alloy

3. Indentation

A vital prerequisite for microstructure simulation studies is the knowledge of local constitutive behavior of individual phases in the microstructure. Almost all the reported work in micromechanics use the constitutive properties obtained from macroscopic experiments (e.g. tensile test) as the input in FEM calculations. Such phenomenological stress-strain data may not always be representative of the local constitutive behavior of the microstructural volume under consideration. Material microstructures usually span different length scales and structural materials such as metallic alloys/composites have different constitutive behavior at different length scales. Depth-sensing indentation methods, which provide a continuous record of the variation of indentation load as a function of the depth of penetration into the indented specimen, are known to provide reliable measurements or estimates of material mechanical properties (Hay, 2000). These indentation methods are broadly classified into micro- and nano-indentation techniques depending upon the length scale of the indentation depth. They offer an opportunity to study the mechanical properties of a small microstructural volume. Theoretical framework exists to derive mechanical properties such as Young's modulus, yield strength, and strain hardening exponent from the load-depth data (Giannakopoulos, 1999). Detailed scaling and dimensional analysis of the load-depth curve has provided valuable inputs on the dependence of the curve on various mechanical properties such as Young's modulus, Poisson's ratio, yield strength, and strain hardening exponent (Cheng, 2004). Numerical simulation of the load versus penetration depth of indentation using FEM coupled with the experimental data is used in this study to derive the mechanical properties of the Ti-6Al-4V matrix.

3.1 Indentation experiments

Microindentation experiments were carried out using a CSM microindenter which uses a Vickers diamond pyramid, a square pyramid with an included tip angle of 136^0, as the indenter. The equipment allows for either load-controlled or depth-controlled experiments. The exact location where the indentation needs to be performed can be selected using the microscope attached to the equipment. In the current study, depth-controlled indentations of 5μm depth were performed on the T-6Al-4V matrix region of the extruded Ti-6Al-4V-1B alloy. The loading and unloading rates were kept the same at 1N/minute. Figure2 shows the optical micrograph of the residual indent on the sample and the corresponding load-depth curve. The load-depth curves for different indents on the same sample are expected not to be exactly the same as it depends on the local variations in the microstructure. Hence to obtain the average local mechanical response of the Ti-6Al-4V alloy, twelve indentations were carried out on the sample and the results were averaged.

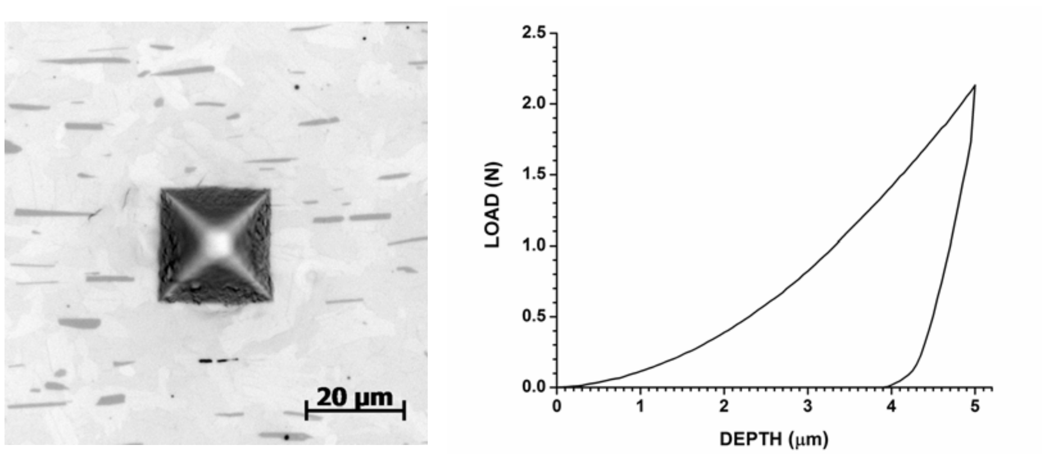

Figure 2. (a) Residual indent on Ti-6Al-4V and (b) the corresponding load-depth curve

3.2 Finite element model of indentation

The local mechanical properties of Ti-6Al-4V alloy are estimated by solving the inverse problem via FEM where the material constitutive properties in the FE indentation model are incrementally varied until the simulated load-depth curve matches the experimental curve. The material constitutive properties that lead to such an agreement can be considered as representative of the local material behavior and can be used as the input in FE based micromechanical studies. It has been reported in the literature, and also verified by the authors, that the Vickers pyramid and an equivalent cone having the same projected area as the pyramid will essentially show the same load-depth response. This enables the use of an axisymmetric 2D model in the FE studies to simulate the experimental load-depth curve using a Vickers indenter. The indentation experiment was modeled as a static problem. Nonlinear geometry (NLGEOM) was activated to account for the large strains experienced in the sample immediately underneath the indenter. The diamond indenter was modeled as a cone with a semi-vertical angle of 70.3^0 which gives the same projected area as the Vickers pyramid. The diamond indenter is assumed to be perfectly elastic with manufacturer supplied properties of elastic modulus E = 1141 GPa, and Poisson's ratio ν = 0.07. The tip of the diamond indenter is never perfectly sharp and it was observed by the authors that with the assumption of a sharp tip, the FE model could not reproduce the experimental load-depth curve irrespective of the material constitutive properties used in the model. The diamond tip was observed under scanning electron microscope and was found to have a tip radius of 2.76 μm. The tip radius was incorporated in the model. The sample was modeled using four nodded axisymmetric quadrilateral elements (CAX4). The constitutive model for the specimen was assumed to be elastic-plastic with power-law hardening plastic behavior. The elastic modulus of Ti-6Al-4V is not expected to change locally and is assumed to be 112 GPa, the experimentally observed value from tensile test. Experimentally observed Poisson's ratio of 0.34 was used. The specimen mesh was refined at the region where it is expected to make contact with the indenter to account for the large stress concentration expected to arise during the indentation. Mesh size of the order of 0.5 μm was used along the contact surface of the specimen. Figure3 shows the indentation model created in ABAQUS. Friction less finite surface-to-surface sliding contact was defined between the bottom of the indenter geometry and the specimen top. Adaptive meshing technique, which allows for remeshing at specified intervals during the analysis, was activated to avoid severe mesh distortion by maintaining a high quality mesh while subjected to large deformation. The indentation experiment was simulated by applying a downward displacement to the indenter which causes the indenter to push into the material to be indented. The bottom side of the sample was pinned to avoid rigid body motion. The load was calculated by summing the reaction forces at the bottom nodes of the indenter. Figure4 shows the von Mises contour plot on the sample during indentation.

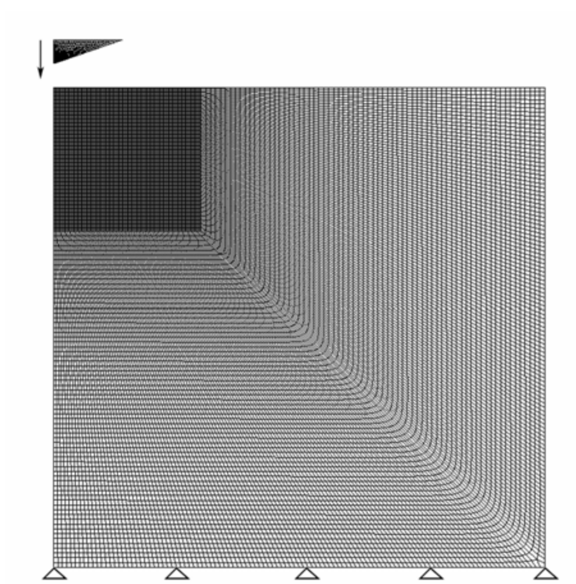

Figure 3. ABAQUS model for microindentation

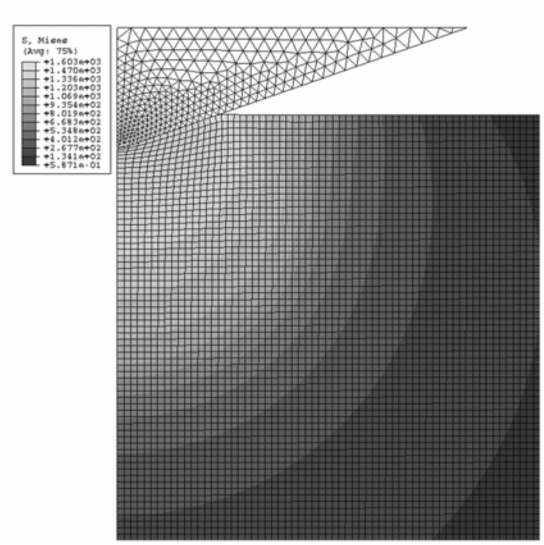

Figure 4. von Mises stress distribution in the sample

The load-depth curve obtained from the model was compared with the experimental curve and the plastic properties of the sample in the model were iteratively modified until both the curves showed a good match. An offset yield strength value of 1050 MPa and a strain hardening coefficient of 0.16 were found to give a good match with the experimental curve. Figure5 shows both the averaged experimental load-depth curve and the simulated curve.

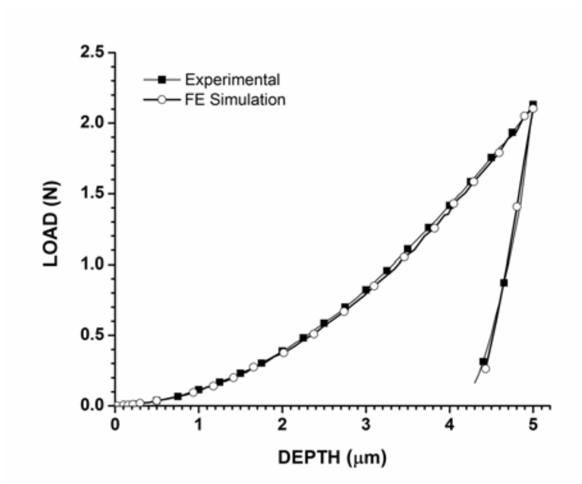

Figure 5. Comparison between the experimental and simulated load-depth curves

Similar studies to determine the elastic properties of the TiB phase were not successful as the load-depth response from the TiB whiskers were found to be affected by the Ti-6Al-4V matrix underneath the whisker. Nanoindentation experiments, with indent depths as low as few tens of nanometers, are expected to give a mechanical response unaffected by the matrix and are currently being investigated by the authors. Wide ranging values, from 350GPa to 485GPa, have been reported for the elastic modulus of TiB in the literature. In the present study, a value of 450 GPa is used as the elastic modulus of TiB.

4. 2-D microstructure modeling and simulations

For microstructure simulations to useful in material development studies, it is essential to be able to conduct parametric studies using realistic phase geometries. A new methodology has been recently developed by the authors' group to simulate realistic material microstructures, details of which can be found elsewhere (Singh, 2006). The methodology involves digitally extracting a large number (~1000) of real TiB whisker high resolution images from the binary image of actual microstructure and using these images to simulate new microstructures with different spatial arrangement of the whiskers, different whisker volume fraction, average size, number density, anisotropy etc. The simulation parameters are verified by using statistical descriptors such as two point correlation functions to compare the real and simulated microstructures. By utilizing the actual whisker morphologies in the simulation, the methodology allows for the creation of 'realistic' virtual microstructures where the simulation parameters may be directly linked to the processing parameters. Figure6(a) shows a portion of the binary image of a simulated microstructure where almost all the TiB whiskers are oriented along the extrusion direction. Figure6(b) depicts a simulated microstructure where all the TiB whiskers are randomly oriented. In reality, this might represent the microstructure of a material which was compacted, but not extruded. Similarly, figure6(c) is a simulated partially anisotropic microstructure that may represent the alloy extruded at a lower temperature and/or a lower extrusion ratio.

All the three microstructures in figure6 were incorporated in an FE framework to study the mechanical response of these materials under uniaxial loading. Since the material microstructures are image files that are of raster format, where the information is stored in pixels, it is not possible to directly import these microstructures into ABAQUS. NIST has developed a public-domain finite element software named OOF (for Object Oriented Finite elements) to mesh and analyze material microstructures (Langer, 2001). OOF allows for directly importing of microstructural images and has a variety of meshing algorithms to mesh the microstructures. In the present study, all the 2D microstructures were meshed using plane stress linear triangular elements (CPS3) in OOF and the mesh was imported to ABAQUS as orphan mesh to carry out the analyses. The microstructures covered an area of 400μm x 400μm and were embedded in a homogenized composite medium. The homogeneous composite medium minimizes the effect of finite boundaries of the model as well as makes it easier to apply the boundary conditions. The FE mesh for all the three microstructures contained over 350,000 elements. The models were analyzed in ABAQUS for elastic-plastic mechanical response under uniaxial loading. The TiB whiskers were assumed to be isotropic perfectly elastic with Young's modulus E = 450 GPa and Poisson's ratio ν = 0.15. The Ti-6Al-4V matrix was assigned an isotropic elastic-plastic behavior obtained from the indentation studies as described earlier. The interface between the matrix and the whiskers was

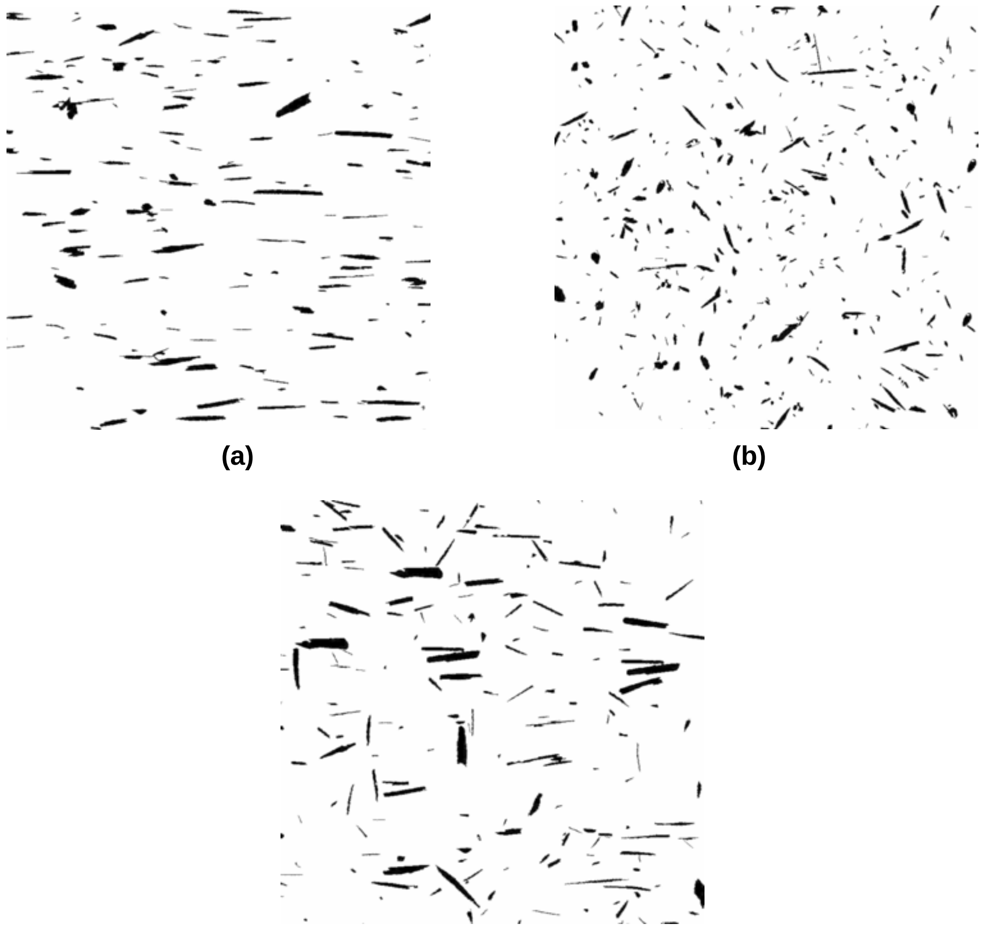

(a) (b)

(c)

Figure 6. Computer simulated microstructures of (a) extruded; (b) compacted; and (c) extruded at a lower temperature and/or a lower extrusion ratio Ti-6Al-4V-1B alloy

assumed to be perfect. Periodic boundary conditions, where the deformation at each boundary is constrained to be equal to that at the opposite boundary, were applied using the EQUATION option in ABAQUS. Uniaxial loading was simulated by applying a displacement so as to produce 2% strain along the extrusion direction. Figure7 shows the FE model along with the boundary conditions. Periodic boundary conditions and the mesh on TiB phase are not marked on the figure for clarity. The displacement needs to be specified only at the bottom right node because of the periodic boundary conditions. Figure8 shows a portion of the FE mesh. It may be observed that the mesh follows the contours of the irregular microstructure and is well refined at the interface between the matrix and the whiskers.

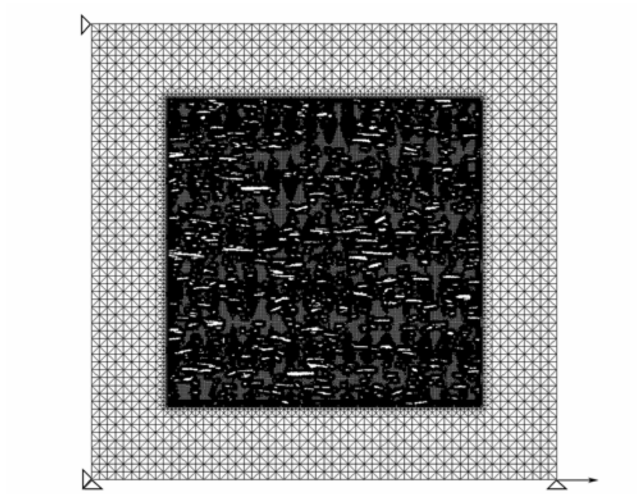

Figure 7. Finite element model for 2-D analysis

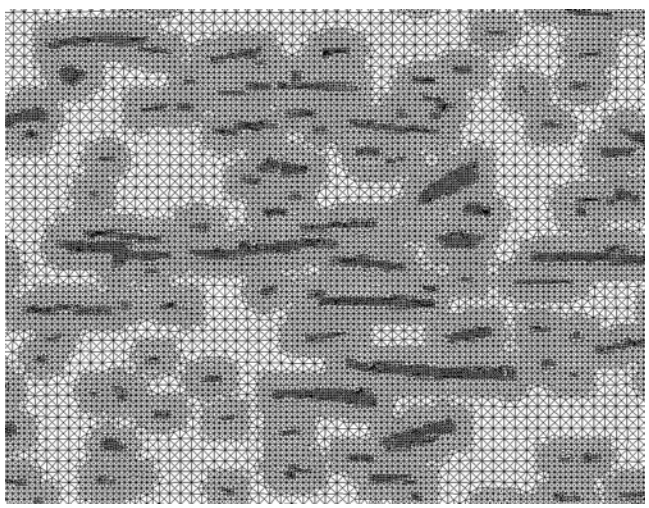

Figure 8. Detail of 2-D finite element mesh

A stress-strain curve was initially assumed for the embedding homogenized medium and was iteratively modified until the calculated stress-strain curve from the embedded cell was identical to that of the embedding medium. The overall stress-strain behavior of the model is obtained by plotting the area averaged reaction force at the bottom right node (where the displacement is applied) versus the strain at the node. Wallclock time for the analyses was approximately 40 minutes. Figure9 shows the contour plot of equivalent plastic strain (PEEQ) distribution in the Ti-

6Al-4V matrix phase under tensile loading. It can be seen that the matrix yielding is the maximum near the TiB whisker tips oriented along the extrusion direction.

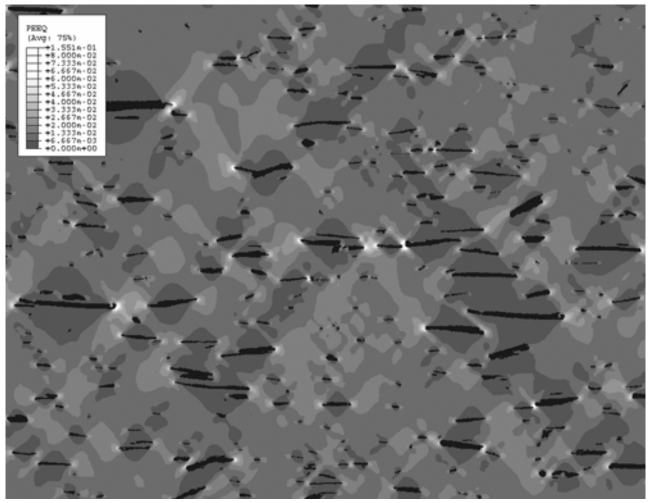

Figure 9. PEEQ distribution in the matrix

Figure10 compares the stress-strain curve obtained from the 2-D simulation with the experimentally observed data for Ti-6Al-4V-1B alloy.

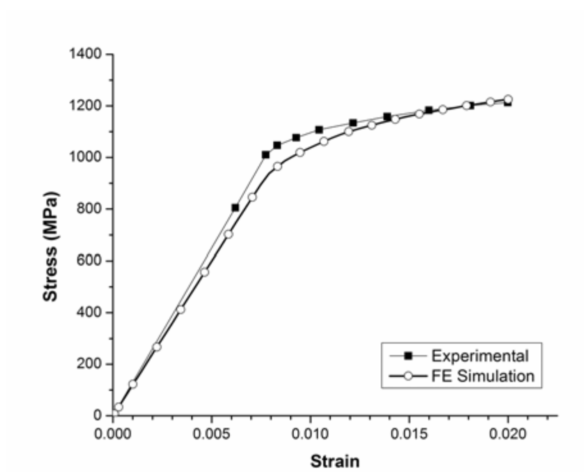

Figure 10. Comparison of experimental and simulated stress-strain curve

Since the same meshing routine was used for all the three microstructures, it is possible to compare the distribution of local maximum principal stress in the TiB whiskers for the microstructures. Figure11 shows the complementary cumulative distribution of local maximum principal stress in the TiB whiskers for the three microstructures. It may be seen that the TiB whiskers are the most effective as a load bearing phase when oriented along the extrusion direction. Such studies can provide useful input for materials design.

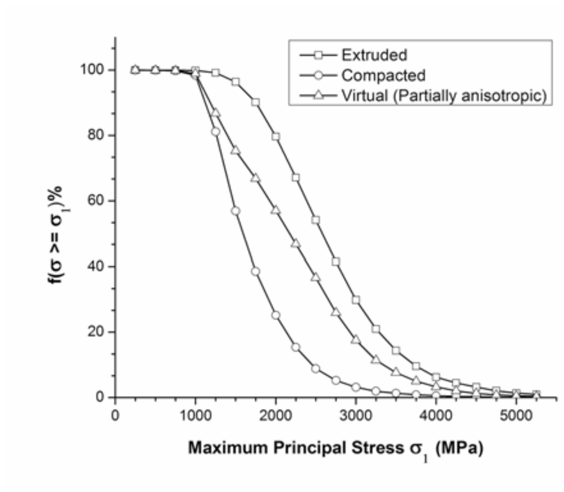

Figure 11. Complementary cumulative distributions of local maximum principal stress in the TiB whiskers under tensile loading for the simulated microstructures

5. 3-D microstructure simulation

Material microstructures are 3-D in nature and 2-D sections do not accurately represent the microstructure in most cases. 3-D microstructure of the Ti-6Al-4V-1B alloy was reconstructed using serial sectioning technique. The metallography and further details can be found elsewhere (Lieberman, 2006). Figure12 shows a digitally rendered 3-D microstructure (100μm × 100μm × 80μm) of compacted and extruded Ti-6Al-4V-1B. The TiB whiskers have anisotropic orientations with the majority of the whiskers aligned parallel to the extrusion direction. While it is possible to directly import the 3-D microstructural volume in any CAD format to ABAQUS directly, the extremely irregular geometry makes it difficult to mesh the volume in ABAQUS. In this study, Harpoon, an automatic hex-dominant mesher for meshing complex 3-D models developed by Computational Engineering International (CEI), was used to mesh the microstructural volume. The reconstructed 3-D microstructure in STL (stereolithography) format was exported into Harpoon and was meshed using a combination of reduced linear hexahedral (C3D8R), tetrahedral (C3D4) and wedge (C3D6) elements. The mesh contained 573,884 elements. The FE mesh was then exported to ABAQUS for further analysis. Uniaxial loading was simulated by applying a strain of 2% along the extrusion direction. The TiB whiskers were assumed to be isotropic perfectly elastic with Young’s modulus E = 450 GPa and Poisson’s ratio ν = 0.15. The Ti-6Al-4V matrix was assigned an isotropic elastic-plastic behavior obtained from the indentation studies as described earlier. The interface between the matrix and the whiskers was assumed to be perfect. Wallclock time for the analysis was approximately 22 hours. Figure13 shows the von Mises stress contour in the model. As could be observed, the TiB whiskers are the primary load bearing phase in the material. Further studies, including application of periodic boundary conditions and obtaining quantitative data from the analysis, are in progress. Research is also underway to develop a methodology to simulate 3-D microstructures with real whisker morphologies in a way similar to the 2-D simulations described earlier.

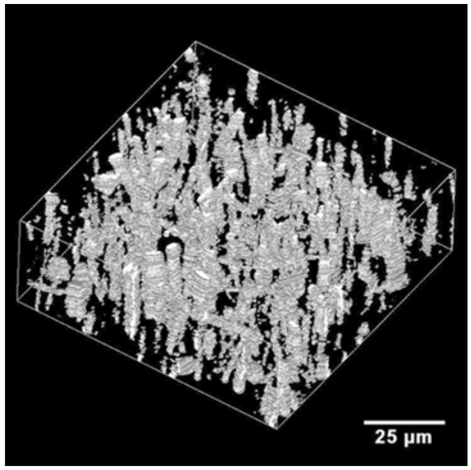

Figure 12. Digitally rendered 3-D microstructure of extruded Ti-6Al-4V-1B alloy

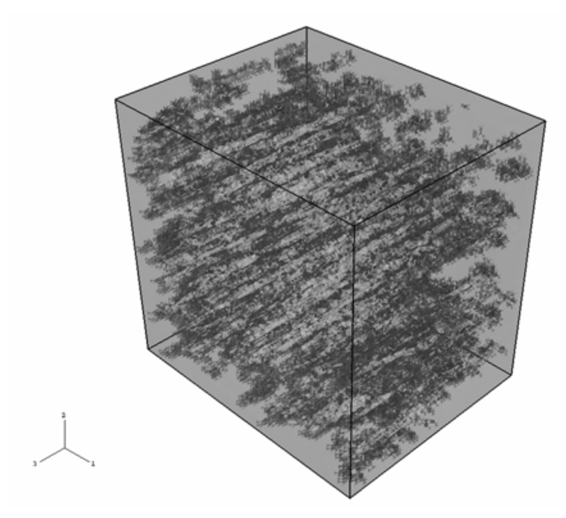

Figure 13. Contour plot of von Mises stress distribution in the model

6. Conclusions

Microindentation experiment, coupled with FE simulations, is shown as a viable option for the calculation of local constitutive properties of material microstructures. The material constitutive properties thus obtained are used as input in realistic microstructure based 2-D and 3-D FE simulations of mechanical response of boron modified titanium alloys. FE simulations are carried out on simulated 'virtual' microstructures that incorporate real phase morphologies. Such studies are shown to provide valuable insight into microstructure-property relationships.

7. References

1. Bao, G., Hutchinson, J. W., and McMeeking, R. M., "Particle Reinforcement of Ductile Matrices against Plastic Flow and Creep," Acta Metallurgica et Materialia, vol. 39, p. 1871, 1991.
2. Cheng, Y. T. and Cheng, C. M., "Scaling, Dimensional Analysis, and Indentation Measurements," Materials Science & Engineering R-Reports, vol. 44, pp. 91-149, AUG 1 2004.
3. Giannakopoulos, A. E. and Suresh, S., "Determination of Elastoplastic Properties by Instrumented Sharp Indentation," Scripta Materialia, vol. 40, pp. 1191-1198, APR 23 1999.
4. Gokhale, A. M. and Yang, S., "Application of Image Processing for Simulation of Mechanical Response of Multi-Length Scale Microstructures of Engineering Alloys," Metallurgical and Materials Transactions A: Physical Metallurgy and Materials Science, vol. 30, p. 2369, 1999.
5. Hay, J. L. and Pharr, G. M., "Instrumented Indentation Testing," in Asm Handbook Volume 8: Mechanical Testing and Evaluation, H. Kuhn and D. Medlin, Eds. Ohio: ASM International, 2000, pp. 232-243.
6. Langer, S. A., Fuller E.R, Jr., and Carter, W. C., "Oof: An Image-Based Finite-Element Analysis of Material Microstructures," Computing in Science and Engineering, vol. 3, p. 15, 2001.
7. Lieberman, S. I., Gokhale, A. M., and Tamirisakandala, S., "Reconstruction of Three-Dimensional Microstructures of Tib Phase in a Powder Metallurgy Titanium Alloy Using Montage Serial Sectioning," Scripta Materialia, vol. 55, pp. 63-68, JUL 2006.
8. Singh, H., Mao, Y., Sreeranganathan, A., and Gokhale, A. M., "Application of Digital Image Processing for Implementation of Complex Realistic Particle Shapes/Morphologies in Computer Simulated Heterogeneous Microstructures," Modelling and Simulation in Materials Science and Engineering, vol. 14, pp. 351-363, APR 2006.

8. Acknowledgement

The authors thank Dr. D. B. Miracle of the Air Force Research Laboratory at Wright-Patterson Air Force Base for providing the Ti-B specimens. This study was supported through research grants from the Air Force Office of Scientific Research (AFOSR grant numbers FA95550-05-1-0062 and F49620-01-1-0045), for which Dr. Brett Conner is the Program Manager. The financial support is gratefully acknowledged. Any opinions, findings, and conclusions or recommendations expressed in this contribution are those of the author and do not necessarily reflect the views of the funding agencies.